International Journal of Pharmaceutics 403 (2011) 237–244

Contents lists available at ScienceDirect

International Journal of Pharmaceutics

journal homepage: www.elsevier.com/locate/ijpharm

Pharmaceutical Nanotechnology

Analysis of lipid nanoparticles by Cryo-EM for characterizing siRNA delivery vehicles

Randy Crawford[a,1], Belma Dogdas[a,1], Edward Keough[b,1], R. Matthew Haas[c], Wickliffe Wepukhulu[c], Steven Krotzer[b], Paul A. Burke[b], Laura Sepp-Lorenzino[b], Ansuman Bagchi[a], Bonnie J. Howell[b,*]

[a] *Informatics IT, Merck & Co, Inc., West Point, PA, USA*
[b] *RNA Therapeutics Delivery Biology, Merck & Co, Inc., West Point, PA, USA*
[c] *RNAi Analytical Sciences, Merck & Co, Inc., West Point, PA, USA*

ARTICLE INFO

Article history:
Received 14 June 2010
Received in revised form
24 September 2010
Accepted 18 October 2010
Available online 23 October 2010

Keywords:
Drug delivery
Liposome characterization
Dynamic light scattering
Oligonucleotides
Nanodrugs
Imaging

ABSTRACT

Lipid nanoparticles are self-assembling, dynamic structures commonly used as carriers of siRNA, DNA, and small molecular therapeutics. Quantitative analysis of particle characteristics such as morphological features can be very informative as biophysical properties are known to influence biological activity, biodistribution, and toxicity. However, accurate characterization of particle attributes and population distributions is difficult. Cryo-Electron Microscopy (Cryo-EM) is a leading characterization method and can reveal diversity in particle size, shape and lamellarity, however, this approach is traditionally used for qualitative review or low throughput image analysis due to inherent EM micrograph contrast characteristics and artifacts in the images which limit extraction of quantitative feature values. In this paper we describe the development of a semiautomatic image analysis framework to facilitate reliable image enhancement, object segmentation, and quantification of nanoparticle attributes in Cryo-EM micrographs. We apply this approach to characterize two formulations of siRNA-loaded lipid nanoparticles composed of cationic lipid, cholesterol, and poly(ethylene glycol)-lipid, where the formulations differ only by input component ratios. We found Cryo-EM image analysis provided reliable size and morphology information as well as the detection of smaller particle populations that were not detected by standard dynamic light scattering (DLS) analysis.

1. Introduction

RNA interference (RNAi) is a highly conserved cellular mechanism which utilizes short double stranded RNA sequences to induce degradation of complementary messenger RNA and inhibit gene expression. RNAi has great potential to manage disease but a major challenge continues to be the reliable and safe delivery of siRNAs to the site of disease (Sepp-Lorenzino and Ruddy, 2008; Whitehead et al., 2009). Numerous technologies are being explored as potential siRNA nanocarriers, among which the encapsulation of siRNAs in Lipid Nanoparticles (LNPs) appears promising. LNP-based techniques are currently the most well-studied siRNA delivery approach for systemic delivery across species, however additional tools are required to quantitatively characterize particle biophysical attributes and correlate them to composition and biological activity. Size, in particular, is one biophysical attribute known to influence multiple factors of nanoparticle-based drug delivery including: particle aggregation properties, opsonization, biodistribution, renal excretion, extravasation from the vasculature, macrophage recognition, complement system activation, cellular fenestration and membrane transport capabilities, surface area related toxicity, as well as drug loading and release properties, with the optimal particle size for drug delivery considered to be in the range of 30–200 nm in diameter (Zhdanov et al., 2002; Emrich and Thanos, 2006; Singh and Lillard, 2009). Both formulation chemistry and formulation process parameters drive final nanoparticle composition, biophysical properties and ultimately biological activity. Because of these intricate relationships between composition, process, biophysical outcome, and biological activity, an accurate quantitative characterization of each is necessary to make statistically significant correlations that drive decision making in drug development.

Biophysical properties have proven to be one of the more difficult for gathering complete quantitative metrics. Several tech-

* Corresponding author at: RNA Therapeutics Delivery Biology, Merck & Co, Inc., 770 Sumneytown Pike, PO Box 4 WP26-462, West Point, PA 19486, USA.
Tel.: +1 215 652 2650; fax: +1 215 993 7490.
E-mail address: Bonnie_Howell@Merck.com (B.J. Howell).
[1] Authors contributed equally to this work.

0378-5173/$ – see front matter © 2010 Elsevier B.V. All rights reserved.
doi:10.1016/j.ijpharm.2010.10.025

niques are often used to assess nanoparticle characteristics such as lamellarity, size, shape, and polydispersity. These include dynamic light scattering (DLS), size exclusion chromatography (SEC), atomic force microscopy (AFM), and Cryo-Electron microscopy (Edwards and Baeumner, 2006). Standard intensity-based DLS measurements have proved to be inadequate in determining the true number-weighted size distribution of heterogeneous liposome populations (Ingebrigtsen and Brandl, 2002; Frantzen et al., 2003). In addition, intensity-weighted *z*-average readouts made by DLS can be biased toward larger particles when measuring heterogenous populations (Berclaz et al., 2001). In a review of multiple studies where the impact of nanoparticle size on drug delivery was investigated by various methods, it was suggested that size measurements reported in these studies often yield incomplete descriptions of the true population size distribution making it difficult to correlate particle size to biological activity (Gaumet et al., 2008). To compensate, a complement of at least one microscopy technique in conjunction with a second standard technique such as DLS has been suggested (Gaumet et al., 2008).

Cryo-Electron Microscopy (Cryo-EM) has become a leading technology for imaging nanoscale biological samples such as lipid nanoparticles. Cryo-EM offers the opportunity to resolve particles of varying sizes, shape, and ultrastructure which may reveal clues to mechanism of action toward the clinical endpoints of efficacy and toxicity. In Cryo-EM imaging, sample processing introduces virtually no structural alterations of the liposome particles under investigation (Almgren et al., 2000) and a true representation of the parent suspension can potentially be captured given proper sample preparation and a sufficient number of particles measured.

Although Cryo-EM analysis has clear advantages, wide adoption of Cryo-EM for nanoparticle characterization has been hindered by several factors such as cost and access to imaging systems, complicated sample preparation, and the low throughput of image acquisition and quantitative image analysis. Whereas greater access to the technology has been afforded through commercial or university Cryo-EM imaging services and both throughput and sample preparation has improved with increased automation, the major bottleneck of quantitative image analysis persists. Typically, analysis of nanoparticles in Cryo-EM images is done manually, which is time consuming and often not quantitative, thereby limiting its potential to generate precise metrics and enable statistical analysis of nanoparticle features. Moreover, Cryo-EM images suffer from significant background noise, nonuniform illumination and artifacts in sample preparation that make consistent automatic identification of particles and subsequent analysis problematic (Tasdizen et al., 2008).

Our objective was to develop a semiautomatic image analysis framework to facilitate reliable image enhancement, object segmentation, and quantification of nanoparticle attributes from Cryo-EM micrographs, and then to apply this methodology to accurately characterize and differentiate nanoparticles on size and morphology. To achieve this, we first developed a methodology to enhance, denoise, and segment LNPs from Cryo-EM images. This allowed us to overcome impediments to conventional analysis and to facilitate a higher throughput quantitative analysis of the particles. We then show application of the methodology to two LNP formulations where the cationic lipid, cholesterol and poly(ethylene glycol) (PEG) in the siRNA-loaded lipid nanoparticles were investigated at mole ratios of 60:38:2 and 74.6:20:5.4 respectively. We performed standard intensity-weighted DLS measurements on the same lipid nanoparticle samples and compare these results to those obtained through Cryo-EM analysis, illustrating the advantages of Cryo-EM analysis to accurately characterize and differentiate formulations based on biophysical properties.

2. Materials and methods

2.1. Materials

Lipid nanoparticles were assembled from a mixture of the following lipids: CLinDMA (2-{4-[(3β)-cholest-5-en-3-yloxy] butoxy}-*N*,*N*-dimethyl-3-[(9*Z*,12*Z*)-butyl-9,12-dien-1-yloxy]propan-1-amine), cholesterol, and polyethylene glycol-dimyristoylglycerol (alpha-[8′-(1,2-dimyristoyl-3-propanoxy)-carboxamide-3′,6′-dioxaoctanyl]carbamoyl-omega-methyl-poly(ethylene glycol)$_{2000}$). Cholesterol was purchased from Northern Lipids (Burnaby, BC, Canada). Cationic lipid, poly(ethylene glycol)-lipid (PEG), and siRNA sequences were synthesized by Merck and Co., Inc. (West Point, PA) as described previously (Wincott et al., 1995; Morrissey et al., 2005).

2.2. Preparation of LNP formulations

siRNAs were encapsulated into lipid nanoparticles as previously described (Abrams et al., 2009) in two formulation batches using identical sample preparation. One batch contained a composition of cationic lipid:cholesterol:PEG at a 60:38:2 mole ratio to generate a "low-PEG/high-cholesterol" formulation and a second batch contained a 74.6:20:5.4 mole ratio of cationic lipid:cholesterol:PEG to generate a "high-PEG/low-cholesterol" formulation of siRNA containing lipid nanoparticles.

2.3. Dynamic light scattering (DLS)

Lipid nanoparticle formulations were diluted to a siRNA concentration of 10–30 μg/ml in sterile 6 mM sodium phosphate buffer, pH 7.5. Size was measured in triplicate using a Zetasizer Nano ZS (Malvern Instruments, Worcestershire, United Kingdom) and reported as Z-average diameter. The intensity-weighted size distribution as reported by the instrument was transformed into a number-weighted size distribution by the instrument software for our purposes of comparing the DLS results to the sizes generated from Cryo-EM micrographs.

2.4. Cryo-EM grid preparation and image acquisition

Cryo-EM images were acquired by Nano Imaging Services (San Diego, CA). Vitrification (rapid freezing) of undiluted lipid nanoparticle sample was performed using an FEI Vitrobot operating at 4 °C, 95% RH with sample suspensions supported on a C-Flat holey carbon film (Protochips, Inc., Raleigh, NC). Carbon films were supported by a 400 mesh copper grid that had been plasma cleaned. After vitrification, sample grids were maintained at a temperature below −170 °C at all times. Imaging was performed on an FEI Tecnai T12 transmission electron microscope operating at 120 keV equipped with an FEI Eagle 4K × 4K CCD camera. Image locations were selected with the intention of capturing the best distribution of particle sizes in the holes of the carbon film where nanoparticles are trapped and often size-sorted in ice, with additional images collected from various regions of the carbon film. Pairs of images in approximately 20 locations per sample were acquired at magnifications of 52,000× (0.21 nm/pixel) and 21,000× (0.50 nm/pixel). The images were acquired at a nominal underfocus of −5 μm (21,000×) and −4 μm (52,000×) with electron doses of ~10–15 $e^-/Å^2$.

2.5. Preprocessing and segmentation of Cryo-EM micrographs

Cryo-EM images captured at 52,000× magnification were qualitatively selected for analysis with the intention of capturing at least 200 lipid nanoparticles per sample to be processed by our custom

MATLAB tool. We implemented a series of automated image processing steps in MATLAB (The MathWorks, Natick, MA), including illumination correction, filtering and denoising, contrast enhancement, and segmentation of lipid particles in Cryo-EM micrographs. The product was a binary particle segmentation denoting the body of each visible nanoparticle. Occasional errors in image segmentation occurred and were compensated through the exposure of approximately six control parameters within the particle denoising, contrast enhancement, and segmentation processes, and the manual adjustment of these values to tune the results. We also developed an interactive segmentation editor (ISE) implemented in MATLAB to correct segmentation errors that were not compensated by prior control parameters and produce a final, highly accurate segmentation mask for analysis. This tool is described in more detail in Section 3.

2.6. Extraction of particle attributes

The corrected nanoparticle segmentation masks were utilized for the extraction of particle metrics within the Acapella software system (PerkinElmer, Waltham, MA) designed for analysis of high-content cellular imagery. We developed a morphometric analysis script in Acapella to use a nuclear segmentation algorithm to assign the particles from the MATLAB-generated segmentation mask to an object list, overlay this stencil with the MATLAB-enhanced Cryo-EM micrograph, and calculate multiple image measurements on a particle-by-particle basis. These metrics, including particle area, perimeter length, major axis length, particle roundness and X/Y coordinates, were computed and converted from pixel to true nanometer units. Through Acapella all image sets were batch analyzed with identical algorithm parameters and a single master table of results was generated containing particle-by-particle data for both of the LNP formulations. Subparticle metrics of LNPs such as object contrast levels and identified substructures were also extracted by the analysis script but are not included in this manuscript. For our size metric, each particle was assumed to be circular and the equivalent circular diameter was calculated from the particle area measurement. The elongation metric was then calculated as the ratio of the major axis length to the equivalent circular diameter.

3. Results

3.1. Dynamic light scattering of lipid nanoparticles

siRNAs were encapsulated in lipid nanoparticles at two different input mole ratios of cationic lipid, cholesterol, and PEG, as described in Section 2. Dynamic light scattering (DLS) was used as a routine method to gather information on mean particle size and polydispersity. The low-PEG/high-cholesterol formulation, consisting of a 60:38:2 mole ratio of cationic lipid, cholesterol, and PEG resulted in a DLS number-weighted mean diameter of 96.6 nm and intensity-weighted z-average diameter of 120.1 nm with a polydispersity index (PDI) of 0.075. The DLS measurement for the high-PEG/low-cholesterol formulation with a composition ratio of 74.6:20:5.4, was about 50% smaller at 48.1 nm number-weighted mean diameter and 63.3 nm intensity-weighted z-average with a PDI of 0.083 (see Fig. 1 and Table 1). A single peak is observed in the size distribution for both formulations and the two PDI values are relatively comparable and indicate these samples are nearly monodisperse.

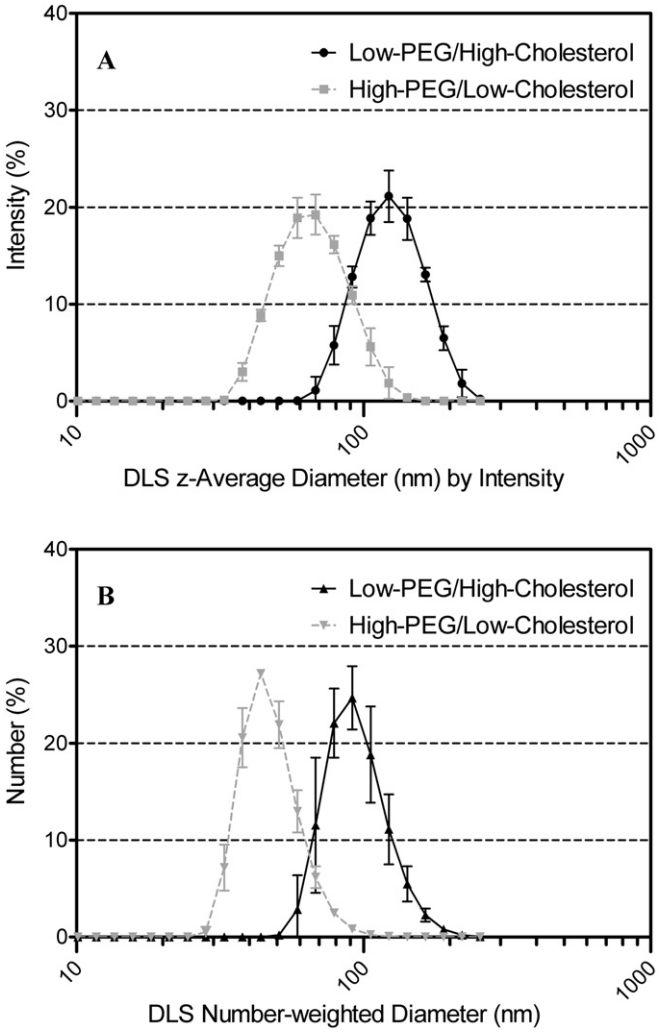

Fig. 1. (A) Intensity-weighted DLS diameter measurement of low-PEG/high-cholesterol composition (●) and high-PEG/low-cholesterol composition (■) lipid nanoparticle formulations. (B) Number-weighted DLS diameter measurement of low-PEG/high-cholesterol composition (▲) and high-PEG/low-cholesterol composition (▼) lipid nanoparticle formulations. Error bars show standard deviation between three repeat measurements.

3.2. Cryo-EM image acquisition and selection of images for analysis

Next, we wanted to compare the DLS findings with those obtained via Cryo-EM. To begin, Cryo-EM images were selected for quantification with the goal of generating particle size and shape attributes for a minimum of 200 particles per sample. Images

Table 1
Number-mean diameter and z-average diameter in nanometer and polydispersity index obtained by intensity-weighted DLS measurement and mean geometric circular diameter in nanometer obtained by Cryo-EM image analysis. Standard deviation (SD) values in parenthesis are in nanometer units for three repeat DLS measurements and in nanometer units for geometric standard deviation in Cryo-EM measurements.

Measurement	Low-PEG/high-cholesterol composition	High-PEG/low-cholesterol composition
DLS number-mean diameter in nm (SD)	96.6 (6.6)	48.1 (1.4)
DLS z-average diameter in nm (SD)	120.1 (1.7)	63.3 (0.8)
DLS polydispersity index (SD)	0.075 (0.054)	0.083 (0.039)
Cryo-EM mean geometric circular diameter in nm (SD)	55.0 (1.6)	35.0 (1.3)

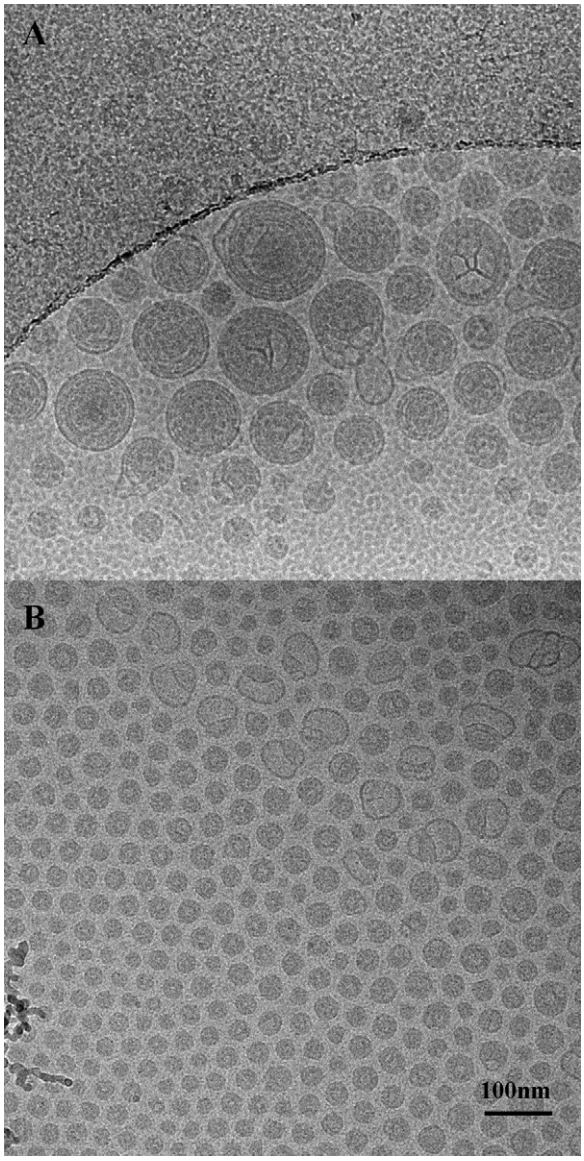

Fig. 2. Cryo-EM images at 52,000× relative magnification as captured on FEI Tecnai T12 transmission electron microscope for low-PEG/high-cholesterol composition (A) and high-PEG/low-cholesterol composition (B) of lipid nanoparticles.

displaying the majority of a carbon hole were preferred because the vitrified aqueous film in this region forms a layer of steadily increasing thickness from center to edge in the hole of the carbon film allowing both smaller and larger particles from the parent suspension to be visible. Where possible, images containing significant particulate artifacts were avoided but in some cases were simply manually excluded using our down-stream analysis tools. Fig. 2A shows a representative 52,000× Cryo-EM image of the low-PEG/high-cholesterol nanoparticle formulation in this study and reveals a diversity of LNP sizes, shapes and lamellar properties within a single population. For example, most low-PEG/high-cholesterol particles in this image demonstrate a uniform distribution of multilamellar substructure whereas others have internal void spaces and/or elongated protrusions extending from their outer surface. In contrast, Fig. 2B shows the high-PEG/low-cholesterol formulation where nanoparticles appear smaller in size and have a less distinguishable lamellar substructure, yet still have considerable diversity of particle characteristics.

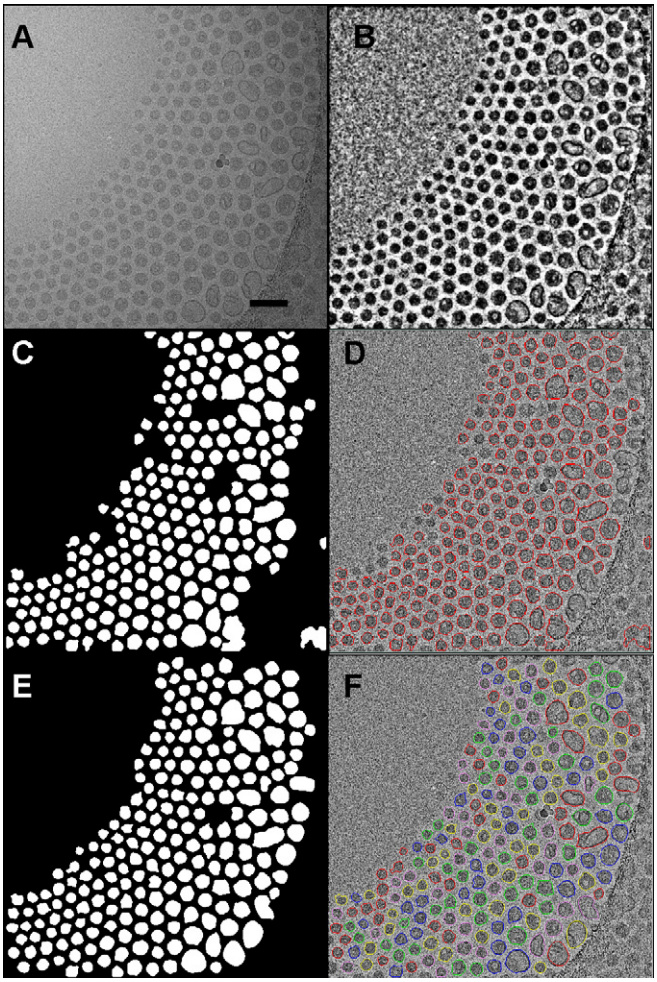

Fig. 3. Overall MATLAB and Acapella software workflow showing analysis of 52,000× Cryo-EM image of lipid nanoparticles formulated with high-PEG/low-cholesterol composition ratio. The processes applied to the raw image (A) include: Contrast-Limited Adaptive Histogram Equalization (CLAHE) image enhancement (also see Fig. 4B), FFT and median filters application (B), initial automated particle segmentation in MATLAB to generate a segmentation mask (C), review and editing of particle boundaries in MATLAB Interactive Segmentation Editor (D) for the creation of corrected segmentation mask (E), and Acapella software identification of individual particles (F), followed by data output (scale bar = 100 nm).

3.3. Preprocessing and segmentation of Cryo-EM micrographs

Our first step in performing quantitative image analysis was to adjust for uneven contrast across the images and improve their poor signal to noise ratio. To address this, we initiated a series of image preprocessing steps prior to segmentation of the lipid nanoparticles. Our analysis procedure involved five major steps, as outlined in Fig. 3: (1) compensation for uneven background lighting and contrast enhancement through Contrast Limited Adaptive Histogram Equalization (CLAHE), (2) maximization of relevant signal with minimal loss of detail using median and Fourier transform low pass filters, (3) segmentation of particles using Otsu binary thresholding (Otsu, 1979) and subsequent morphological processing (Haralick et al., 1987). Finally, images were (4) manually reviewed and particle segmentation was corrected using our Interactive Segmentation Editor tool, and (5) particle attributes were extracted as metrics. Steps 1–4 of this workflow were packaged into a pair of MATLAB programs and step five was implemented through Acapella software scripts developed within our lab.

CLAHE (Zuiderveld, 1994) was used to correct uneven background illumination and to enhance contrast in the original

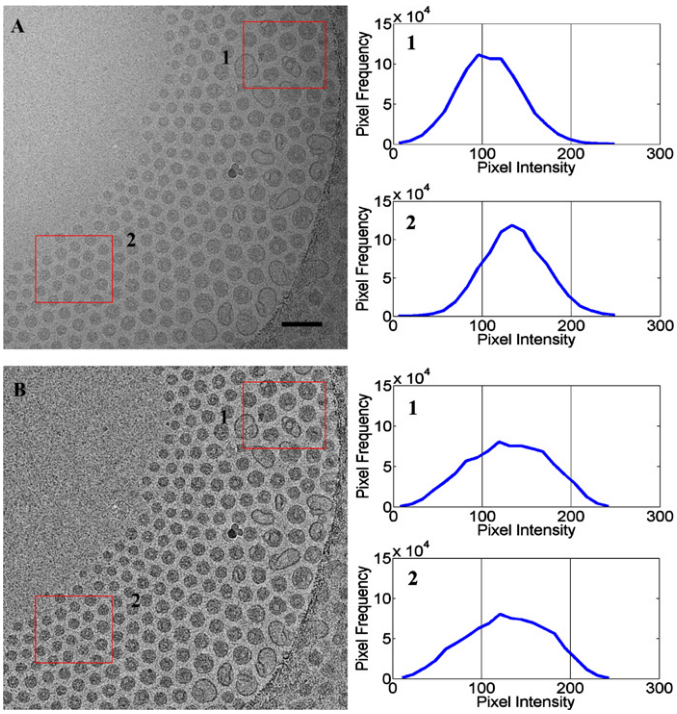

Fig. 4. Raw 52,000× Cryo-EM image of a lipid nanoparticle formulated with high-PEG/low-cholesterol composition ratio (A) corrected for illumination using Contrast-Limited Adaptive Histogram Equalization (CLAHE) (B). Histograms display pixel intensities within the highlighted regions of the image.

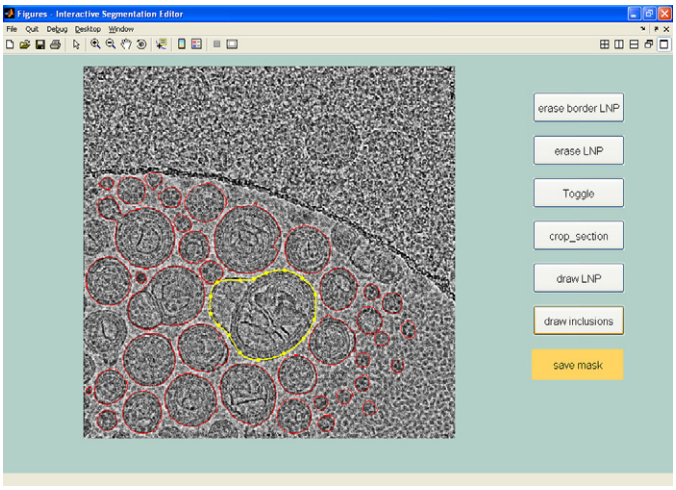

Fig. 5. MATLAB Interactive Segmentation Editor (ISE) window display. A full-scale image from the low-PEG/high-cholesterol composition is displayed. Particle boundary correction tools are accessed through the buttons on the right. In the center of the image is a particle undergoing manual correction.

Cryo-EM image (see Fig. 4A). In Adaptive Histogram Equalization (AHE), the image is parceled into small patches, performing independent histogram equalizations on each. Dissimilar patches are then reintegrated into a whole using bilinear interpolation to minimize discontinuities. In CLAHE, the contrast gradient within histograms is also limited to minimize noise amplification in homogeneous regions. In our code, both a full-resolution CLAHE enhanced image at 4096 × 4096 pixels (see Fig. 4B) and an eightfold reduced image at 512 × 512 pixels were generated. The eightfold reduced image was preferred for speed when computing morphology metrics and segmentation, where the higher-resolution enhanced image was reserved for presentation and subparticle measurement. Fig. 4 illustrates background illumination correction using CLAHE. In Fig. 4A, pixel intensity histograms of two selected regions in a 52,000× image of the high-PEG/low-cholesterol lipid nanoparticle sample show a shift in intensity peaks that demonstrates the variation in signal intensity throughout the image due to uneven illumination. Fig. 4B shows the compensating effects of applying CLAHE – nanoparticles are of higher contrast to local background and contrast is normalized across the image. One advantage of this approach is that multiple images taken from the same sample, even with different magnifications, will have relatively consistent particle-to-background contrast after CLAHE, allowing more accurate automated segmentation later.

To further enhance the images before segmentation, we also applied a low pass Fourier transform filter and a median filter (Gonzalez and Woods, 2008) to the image after CLAHE enhancement to remove background noise that may have arisen due to CLAHE (see Fig. 3B). A global intensity automated thresholding method (Otsu's thresholding) was then applied to separate particles from background by determining an intensity threshold such that the combined background-to-particle variance is maximized (Otsu, 1979). After segmentation, the resultant binary mask contained holes and disconnected regions due to intensity variations within the particles. The discontinuous regions were then integrated by applying a morphological closing operation resulting in a useful segmentation mask (see Fig. 3C) (Haralick et al., 1987). Because a wide variety of particle morphologies and packing densities can be expected when evaluating large numbers of Cryo-EM images generated from many lipid nanoparticles formulations, several filter and process parameters were integrated as user-configurable input variables. These include: minimum and maximum particle size, a particle density filter, and several particle shape filters. By packaging these processes into a MATLAB program, image enhancement and initial automated segmentation required less than one minute per image and was performed in batch on multiple images.

Due to the variety of shapes and sizes of LNPs as well as inherent image artifacts, automatic segmentation did not always accurately outline all particles in the images (see Fig. 3C and D). Hence we needed a means to manually correct those particles that were poorly segmented. To this end, we created an Interactive Segmentation Editor (ISE) in MATLAB to review and edit the automatically generated particle segmentation mask. The ISE's graphical user interface (see Fig. 5) allows the user to load the CLAHE enhanced grayscale image along with the auto-generated particle segmentation mask, overlay the two images, and perform various operations to manually revise the segmentation mask. When the user loads a mask, each particle in the mask is converted from a solid object into a color outline, which is overlaid onto the enhanced grayscale image for reference of the underlying particles' boundaries. Using a mouse or a touch-screen stylus, the user can then select a number of existing particles for deletion, define an arbitrary region for erasure of all particles inside this region, adjust the margins of inadequately segmented particles, and/or outline a new particle. A new mask for each particle is defined via a succession of mouse clicks along the particle's periphery denoting its boundary points, to which a curved line is then fitted using splines. This process of performing quality control of segmentation requires 1–5 min per image depending on the success of initial automatic segmentation, the quality of the image, and the number of particles in each image. Once the corrections are finished, the "corrected mask" (see Fig. 3E) is saved and this updated segmentation mask is utilized for highly accurate particle identification and measurement.

3.4. Extraction of particle attributes

Although our MATLAB application has the ability to extract particle metrics from the segmentation mask, we chose to use Acapella software for nanoparticle quantification due to its powerful suite of microscopy image analysis algorithms and its flexibility for custom script development. After generation of the MATLAB corrected segmentation mask, we applied our custom Acapella analysis script to identify individual particles (see Fig. 3F) and calculate multiple measurements on a particle-by-particle basis. Measurements included particle area, perimeter length, major axis length, roundness, and *X*/*Y* coordinates. All images were analyzed in a batch process using identical algorithm parameter settings. A single master table of particle-by-particle results was generated along with a final fused image of numbered outlined particles overlaying the MATLAB enhanced image for cross-referencing the numerical data to the particle image. Histograms and scatter plots for each measurement were created using GraphPad Prism (GraphPad Software Inc., La Jolla, CA) and Spotfire DecisionSite software (TIBCO Software Inc., Palo Alto, CA), respectively, from the particle-by-particle numerical results.

For this work, we extracted 251 particles from 9 images of low-PEG/high-cholesterol sample, and 868 particles from 5 images of high-PEG/low-cholesterol. Our Acapella scripts analyzed these 14 images in less than 5 min. For the low-PEG/high-cholesterol formulation, the geometric mean particle circular diameter by Cryo-EM was calculated as 55.0 nm with a geometric standard deviation of 1.6 nm, and the population distribution profile was broad. For the high-PEG/low-cholesterol formulation, the geometric mean particle diameter was 35.0 nm with geometric standard deviation of 1.3 nm and this formulation resulted in a more narrow distribution profile compared to the low-PEG/high-cholesterol formulation (see Table 1 and Fig. 6A). 5 particles from the low-PEG/high-cholesterol formulation and 3 particles from the high-PEG/low-cholesterol formulation were larger than the range of the graph's *x*-axis. Particle elongation and circular diameter were plotted on a particle-by particle basis (see Fig. 6C). The high-PEG/low-cholesterol formulation had a slightly higher fraction of elongated nanoparticles compared to the low-PEG/high-cholesterol formulation.

Some literature has indicated the number of particles needed for quantification can be quite high in order to adequately represent the particle size (diameter) distribution in microscopy image analysis (Beekman et al., 2005; Paine, 1993). First, we note the sample sizes chosen for our evaluations were reasonable (based on methodology described in Vigneau et al., 2000, the width of 95% confidence bands were just 0.085 for of low-PEG/high-cholesterol, and 0.046 for of high-PEG/low-cholesterol). Furthermore, to determine whether we have counted sufficient number of particles for each formulation, we compared sample particle distribution characteristics with varying sample size. We randomly selected 100 samples of sizes 25, 50, 75, . . ., 250 for low-PEG/high-cholesterol and 50, 100, 150, . . ., 800 for high-PEG/low-cholesterol formulations and computed average geometric standard deviations (see Fig. 7). In both cases, the average standard deviation values quickly stabilized (and the error bars around the average values steadily decreased) with increasing sample size. Additionally, we evaluated intra-sample differences in particle size distributions by computing the D-statistics via the two sample Kolmogorov–Smirnov (KS) test (Vigneau et al., 2000). Once again, sample-to-sample differences became statistically insignificant ($p < 0.05$) at a sample size of 100 or more, irrespective of the formulation (see Fig. S1 in the Supporting Material). Collectively these observations imply that the sample of particles chosen for our Cryo-EM experiments were appropriate to measure the whole population characteristics for each formulation.

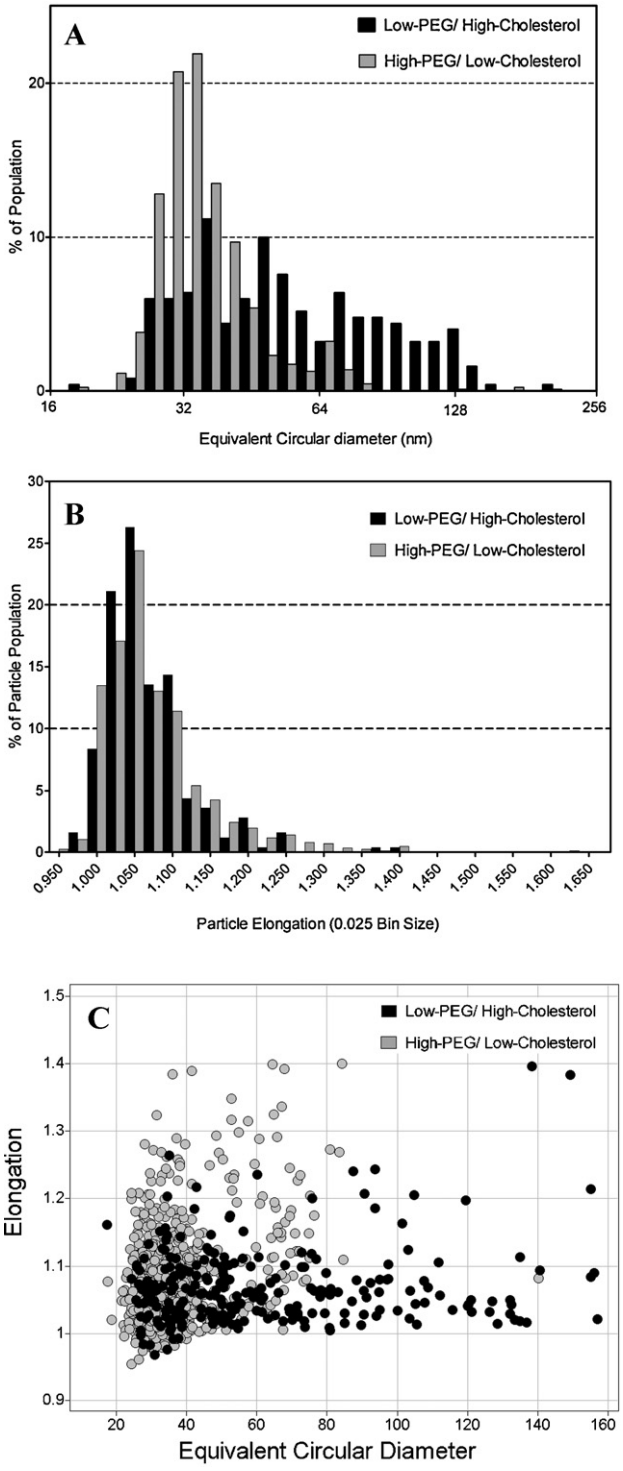

Fig. 6. Histograms of particle equivalent circular diameter (A) and elongation (B) derived from Cryo-EM image analysis for low-PEG/high-cholesterol composition and high-PEG/low-cholesterol composition of lipid nanoparticles. A scatter plot of particle-by-particle results for these two metrics follows (C).

4. Discussion

Synthetic lipid nanoparticles have been widely studied for scientific and medical applications (Müller et al., 2000; Prow, 2004; Whitehead et al., 2009). When designing novel nanoparticles, one must consider how biophysical properties of particles (e.g. size, uniformity, surface area, etc.) impact biological function. Several methods can inform on nanoparticle size, lamellarity, and poly-

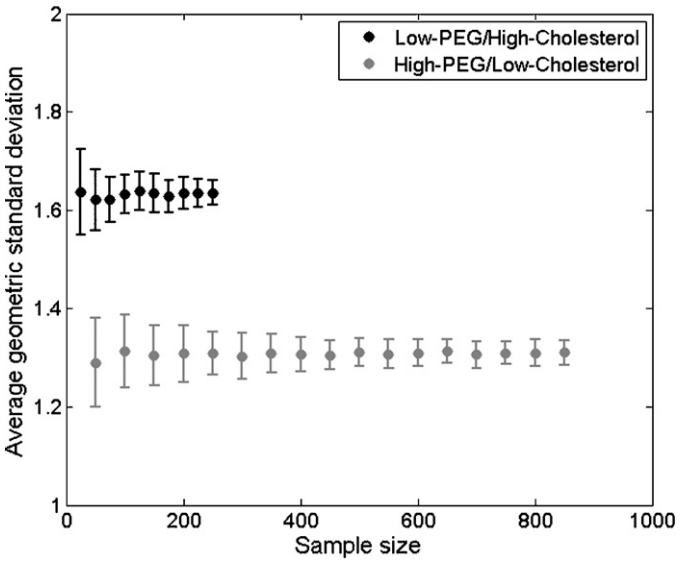

Fig. 7. Effect of varying sample size on the computed average geometric standard deviation over randomly selected 100 samples of sizes 25, 50, 75, . . ., 250 for low-PEG/high-cholesterol composition and 50, 100, 150, . . ., 800 for high-PEG/low-cholesterol composition of lipid nanoparticles.

dispersity, however some of these approaches are limited in the number of readouts they provide and thus require the use of supplemental technologies. Moreover, many of these technologies are limited in their ability to accurately report on biophysical properties because of population heterogeneity. Approaches like DLS are used frequently to determine nanoparticle size and polydispersity and offer advantages of high-throughput, low cost, and minimal sample handling. Non-automated DLS readers can measure single samples in ~10 min and high-throughput DLS readers can measure samples within ~1 min. DLS, however, traditionally uses an intensity-weighted calculation based on an equivalent sphere principle in which each particle is represented as a sphere, thus the existence of aggregates in the sample preparation can excessively increase readout of mean size (Ingebrigtsen and Brandl, 2002; Edwards and Baeumner, 2006). Furthermore, factors such as temperature, concentration, particle sedimentation, and the pH and viscosity of the buffer can also influence DLS size and PDI measurements (Ingebrigtsen and Brandl, 2002; Gaumet et al., 2008). Use of a variable angle light scattering system can improve accuracy of size measurements; however reliability is still a concern when analyzing samples with mixed population of sizes (Gaumet et al., 2008; Borkovec, 2002). DLS also lacks the ability to report on lamellarity and morphology.

Cryo-EM, on the other hand, has several advantages in that it offers nanoscale visualization of individual lipid nanoparticles and provides both size and morphological information. Cryo-EM, however, still lacks wide-spread adoption for liposome analysis due to sample preparation complexity, cost, limited throughput, and the absence of quantitative image analyses tools. In general, artifacts introduced by Cryo-EM imaging or sample preparation, such as uneven image contrast, low contrast of nanoparticles to background, noise from the vitrified film thickness or carbon hole edge, and particulate contaminants, complicate the ability of fully automated software to accurately segment nanoparticle boundaries. Some of these problems have been overcome through careful attention to methodology and automation, as described in a recent review of cryo-electron microscopy of liposomes (Frederik and Hubert, 2005), whereas other bottlenecks still need to be addressed through advances in image analysis methods and software. Therefore, the goal of this work was to fill the void of quantitative image analysis by developing a semiautomated Cryo-EM micrograph analysis framework for extracting particle attributes, and to demonstrate the successful application of this framework through the characterization of siRNA-loaded lipid nanoparticle samples that differ only in their formulation component mole ratios.

The Cryo-EM framework described here enhances Cryo-EM micrographs, segments out individual lipid nanoparticles particles, and provides a semi-automated framework for quantitative image analysis of particle morphology attributes. This approach allows us to improve image quality as well as normalize the images for intensity and contrast before applying a flexible and familiar image analysis routine for quantification. Together these tools more accurately detect and report nanoparticle properties and better assess biophysical particle attributes with improved throughput over manual measurements.

Using our image analysis framework, we compared our Cryo-EM metrics to those obtained by DLS for two nanoparticles with identical chemical components at different mole ratios. One notable difference that emerged from our comparison was the average reported size of the particles. Depending on the DLS method utilized, we found DLS measured sizes to be 30% to >100% larger than those obtained by Cryo-EM for the same liposome formulation. In DLS, the *z*-average size (diameter in nm) is calculated from the intensity weighted average hydrodynamic size of the particles and strongly influenced by complexities of the particle surfaces (Edwards and Baeumner, 2006). Because scattering intensity is proportional to the square of the particle molecular weight, any polydispersity or breadth in particle size distributions will bias the *z*-average toward larger particle sizes (Ingebrigtsen and Brandl, 2002; Edwards and Baeumner, 2006). Thus, the mean diameter obtained from Cryo-EM and DLS techniques will be similar only if the distribution is monomodal and monodisperse. In the examples shown here, the DLS polydispersity value of about 0.08 for both formulations was not very informative of the differences in particle populations, as evident from the Cryo-EM images. Moreover, the low-PEG/high-cholesterol formulation showed a very broad distribution in particle sizes by Cryo-EM analysis, with >90% of the population ranging from ~20 to 110 nm where intensity-based DLS measurements recorded <60% of the particle population falling into this range and no particles under 60 nm. By Cryo-EM, >90% of particles from the high-PEG/low-cholesterol formulation showed a tight distribution and ranged from 20 to 50 nm where intensity-based DLS measurements indicated <30% of the particles from the same formulation fell into this size range. We attribute the absence of the smaller particles (by Cryo-EM observation) in our DLS measurements to be due to a bias of DLS toward measuring larger particles in a heterogeneous lipid nanoparticle population (Berclaz et al., 2001). Number-weighted correction of the intensity-based DLS measurements resulted in particle size predictions closer to the Cryo-EM size measurements, however still failed to accurately account for the smallest particles in the population. Using a number-weighted DLS approach, <1% of the low-PEG/high-cholesterol formulation population was under 50 nm in size and <1% of the high-PEG/low-cholesterol formulation was under 30 nm in size. Cryo-EM showed nearly 50% of the low-PEG/high-cholesterol formulation population under 50 nm in size and nearly 30% of the high-PEG/low-cholesterol formulation under 30 nm. Understanding true particle size and population heterogenity for drug delivery vehicles could enhance interpretation of biological outcome as influenced by nanocarrier biophysical properties. As reported by either DLS or Cryo-EM measurements, the low-PEG/high-cholesterol formulation resulted in particles that were 50-100% larger on average than particles in the high-PEG/low-cholesterol liposome formulation. Interestingly, the differences in size distributions observed here arose from minor changes in lipid ratios despite identical chemical components, highlighting the rele-

vance of subtle compositional changes on nanoparticle biophysical properties and on (potential) biological impact.

An additional benefit of Cryo-EM is the gained insight it offers into particle shape and substructure. Since morphology, lamellarity, and substructure of lipid nanoparticles can vary significantly due to lipid composition and preparation procedures, and can range from unilamellar to multilamellar, round to elongated, and smooth to an irregular complex substructure, Cryo-EM offers an advantage over DLS (Edwards and Baeumner, 2006). For the two formulations investigated here, both displayed similar elongation profiles in our Cryo-EM analysis; however the particles in the low-PEG/high-cholesterol formulation were found to be slightly more spherical than the high-PEG/low-cholesterol formulation, and some particles in both preparations contained obvious void areas and protrusions from the particle surface. These void regions and extended protrusions, in addition to the complex lamellar substructure, are intriguing. Work is ongoing in our labs to develop software applications which examine the relationship of particle size, lamellarity, and substructure to biological function.

To conclude, lipid nanoparticles are self-assembling, dynamic structures in which biophysical properties and biological function can be controlled, in part, through formulation and composition. In this report, we presented techniques and methods for nanoparticle recognition, feature extraction, and the quantitative assessment of particle morphology using our semiautomated image analysis framework that enhances, denoises, segments, and measures lipid nanoparticles in Cryo-EM images. Our system provides the means to extract metrics of nanoparticle features using a high-content analysis approach to quantitatively compare formulation with biophysical traits and biological function and shows advantages over standard dynamic light scattering approaches.

Acknowledgements

The authors acknowledge Seungtaek Lee (PerkinElmer Life and Analytical Sciences) for his assistance in the development of the Acapella software script for Cryo-EM image analysis. We thank Dave Boyd (Merck and Co., Inc.) for his contribution to lipid nanoparticle formulation. In addition, the authors acknowledge Jason Murphy, Anthony Leone, Lou Crocker, James Cunningham, Dave Mathre and Alan Sachs (Merck and Co., Inc.) for supporting this work and providing input on the manuscript.

Appendix A. Supplementary data

Supplementary data associated with this article can be found, in the online version, at doi:10.1016/j.ijpharm.2010.10.025.

References

Abrams, M.T., Koser, M., Seitzer, J., Williams, S.C., DiPietro, M.A., Wang, W., Shaw, A., Mao, X., Jadhav, V., Davide, J.P., Burke, P.A., Sachs, A.B., Stirdivant, S.M., Sepp-Lorenzino, L., 2009. Evaluation of efficacy, biodistribution, and inflammation for a potent siRNA nanoparticle: effect of dexamethasone co-treatment. Mol. Ther. 18, 171–180.

Almgren, M., Edwards, K., Karlsson, G., 2000. Cryo transmission electron microscopy of liposomes and related structures. Colloid Surf. A 174, 3–21.

Beekman, A., Shan, D., Ali, A., Dai, W., Ward-Smith, S., Goldenberg, M., 2005. Micrometer-scale particle sizing by laser diffraction: critical impact of the imaginary component of refractive index. Pharm. Res. 22, 518–522.

Berclaz, N., Blochliger, E., Muller, M., Luisi, P., 2001. Matrix effect of vesicle formation as investigated by cryotransmission electron microscopy. J. Phys. Chem. 105, 1065–1071.

Borkovec, M., 2002. Measuring particle size by light scattering. In: Holmberg, K. (Ed.), Handbook of Applied Surface and Colloid Chemistry. John Wiley, New Jersey, pp. 357–370.

Edwards, K.A., Baeumner, A.J., 2006. Analysis of liposomes. Talanta 68, 1432–1441.

Emrich, D.F., Thanos, C.G., 2006. The pinpoint promise of nanoparticle-based drug delivery and molecular diagnosis. Biomol. Eng. 23, 171–184.

Frantzen, C.B., Ingebrigtsen, L., Skar, M., Brandl, L., 2003. Assessing the accuracy of routine photon correlation spectroscopy analysis of heterogenous size distributions. AAPS PharmSciTec. 4, E36.

Frederik, P.M., Hubert, D.H.W., 2005. Cryoelectron microscopy of liposomes. Methods Enzymol. 391, 431–448.

Gaumet, M., Vargas, A., Gurny, R., Delie, F., 2008. Nanoparticles for drug delivery: the need for precision in reporting particle size parameters. Eur. J. Pharm. Biopharm. 69, 1–9.

Gonzalez, R.C., Woods, R.E., 2008. Digital Image Processing, 3rd ed. Prentice-Hall, Upper Saddle River, NJ.

Haralick, R.M., Sternberg, S.R., Zhuang, X., 1987. Image analysis using mathematical morphology. IEEE Trans. Pattern Anal. Mach. Intell. 9, 532–550.

Ingebrigtsen, L., Brandl, M., 2002. Determination of the size distribution of liposomes by SEC fractionation, and PCS analysis and enzymatic assay of lipid content. AAPS PharmSciTech. 3, E7.

Morrissey, D.V., Lockridge, J.A., Shaw, L., Blanchard, K., Jensen, K., Breen, W., Hartsough, K., Machemer, L., Radka, S., Jadhav, V., Vaish, N., Zinnen, S., Vargeese, C., Bowman, K., Shaffer, C.S., Jeffs, L.B., Judge, A., MacLachlan, I., Polisky, B., 2005. Potent and persistent in vivo anti-HBV activity of chemically modified siRNAs. Nat. Biotechnol. 23, 1002–1007.

Müller, R.H., Mäder, K., Gohla, S., 2000. Solid lipid nanoparticles (SLN) for controlled drug delivery—a review of the state of the art. Eur. J. Pharm. Biopharm. 50, 161–177.

Otsu, N., 1979. A threshold selection method from gray-level histograms. IEEE Trans. Syst. Man. Cybern. 9, 62–66.

Paine, A.J., 1993. Error estimates in the sampling from particle size distributions. Part. Part. Syst. Charact. 10, 26–32.

Prow, T.W., 2004. Nanomedicine: Targeted Nanoparticles for the Delivery of Biosensors and Therapeutic Genes. Ph.D. Thesis. University of Texas, Medical Branch, TX.

Sepp-Lorenzino, L., Ruddy, M.K., 2008. Challenges and opportunities for local and systemic delivery of siRNA and antisense oligonucleotides. Clin. Pharmacol. Ther. 84, 628–632.

Singh, R., Lillard, J.W., 2009. Nanoparticle-based targeted drug delivery. Exp. Mol. Pathol. 86, 215–223.

Tasdizen, T., Jurruss, E., Whitaker, R.T., 2008. Non-uniform illumination correction in transmission electron microscopy. In: MICCAI Workshop on Microscopic Image Analysis with Applications in Biology.

Vigneau, E., Loisel, C., Devaux, M.F., Cantoni, P., 2000. Number of particles for the determination of size distribution from microscopic images. Powder Technol. 107, 243–250.

Whitehead, K.A., Langer, R., Anderson, D.G., 2009. Knocking down barriers: advances in siRNA delivery. Nat. Rev. Drug Discov. 8, 129–138.

Wincott, F., DiRenzo, A., Shaffer, C., Grimm, S., Tracz, D., Workman, C., Sweedler, D., Gonzalez, C., Scaringe, S., Usman, N., 1995. Synthesis, deprotection, analysis and purification of RNA and ribozymes. Nucleic Acids Res. 23, 2677–2684.

Zhdanov, R.I., Podobed, O.V., Vlassov, V.V., 2002. Cationic lipid-DNA complexes-lipoplexes-for gene transfer and therapy. Bioelectrochemistry 58, 53–64.

Zuiderveld, K., 1994. Contrast limited adaptive histogram equalization. In: Heckbert, P. (Ed.), Graphics Gems IV. Academic Press, Boston, MA, pp. 474–485.